

The deflection angle of light by black holes in bumblebee gravity.

Í. D. D. Carvalho ^{1,*}, G. Alencar ^{1,2,†}, W.M. Mendes ^{3,‡} and R. R. Landim ^{1,§}

¹*Universidade Federal do Ceará (UFC), Departamento de Física,
Campus do Pici, Fortaleza - CE, C.P. 6030, 60455-760 - Brazil*

²*International Institute of Physics, Federal University of Rio Grande do Norte,
Campus Universitário, Lagoa Nova, Natal, RN 59078-970, Brazil. and*

³*Departamento de Ensino, Instituto Federal de Educação, Ciência e Tecnologia do Ceará (IFCE),
Campus Crateús, 63700-000, Crateús, CE, Brasil.*

(Dated: February 28, 2025)

In this work, we investigate the influence of the Lorentz symmetry breaking in the bending angle of light for bumblebee black hole solutions. The solutions analyzed break the Lorentz symmetry due to a nonzero vacuum expectation value of the bumblebee field. We use the Ishihara method, which allows us to study the bending angle of light for finite distances and is applicable to non asymptotically flat spacetimes. We consider three backgrounds. The first two are asymptotically flat and were found by Bertolamy *et al* and Casana *et al*. The third was found very recently by Maluf *et al* and is not asymptotically flat due to an effective cosmological constant.

I. INTRODUCTION

The Law of Universal Gravitation was successful in describing the motion of the celestial bodies. Soldner was the first to predict the deflection of light using Newtonian gravity, the corpuscular theory of light, and the fact that light has a finite speed [1]. However, Newton's law of Universal Gravitation did not agree with the experimental data for the perihelion precession of Mercury and the deflection angle of light by Sun. These problems were solved with the emergence of another theory of gravitation, the theory of General Relativity (GR). This theory explained the perihelion precession and predicted a result twice larger to the bending of light. This led to the first of its experimental tests [2]. General Relativity is a classical field theory that considers gravity as a deformation of space-time by matter and energy. This curved space-time determines the particle trajectories [3–6]. As a proof of its predictive power we can mention the detection of gravitational waves in 2016 by the VIRGO and LIGO laboratories [7] and the first photo of a black hole carried out by the EHT project in 2019 [8]. The presence of a distribution of matter and energy leads to a modification of the bending of light, when compared with the empty spacetime case. This bending of light by a distribution of matter and energy is called a Gravitational Lens by analogy with optics (see [9–11] and references therein). The study of Gravitational Lenses is very important because it is a way to investigate many subjects such as: cosmological parameters [12–14], discovery of exoplanets [15, 16] and the investigation of massive compact halo objects (MACHOs) [17].

Beyond gravitation, the physical processes are characterized by the Standard Model (SM), which includes

the electromagnetic, weak and strong interactions. This theory is remarkably successful because it is consistent with almost all experimental results [18] (for a historical review see [19]). However, this theory does not consider the quantum effects of gravitation, and as much as there are several candidates to explain quantum gravity, direct experiments to validate any of those theories are impractical because they are on the Planck scale (10^{19} GeV). However, indirect effects can arise in low energy scales that allow the formulation of experiments. These indirect effects of quantum gravity may be associated with the violation of Lorentz Symmetry. The Standard Model Extension (SME) is an effective theory that generalizes the SM and GR, but this theory allows the violation of the Lorentz and CPT symmetries [20, 21]. A particular SME is the Bumblebee model, which violates the Lorentz symmetry and the diffeomorphism due to a vector field with a nonzero vacuum expectation value [22–24]. Soon later an asymptotically flat black hole solution to the Bumblebee model has been found by Bertolami *et al*. [25]. After this a second static, asymptotically flat solution was found by Casana *et al*. [26]. These results were generalized to stationary spacetimes by Li *et al*. in Ref. [27], which found a Kerr-like black hole solution to the Bumblebee model. Finally, a static, non asymptotically flat solution was found very recently by Maluf *et al*. in Ref. [28].

The Gauss-Bonnet theorem connects differential geometry with topology [29, 30]. In 2008, Gibbons and Werner used this theorem to find a geometrical approach to Gravitational Lens. For this, they consider an optical metric of a weak lensing modeled by a static and spherically symmetric perfect fluid. Their results show that the focusing of light rays arises by topological effects [31]. The extension of this approach was found soon later by Ishihara, where the approximation of infinite distances between the observer-lens-source is not necessary [32]. The fact of considering finite distances enables the method to investigate the deflection of light for geometries which are not asymptotically flat. Finally, Ono *et al*. gener-

* icarodias@alu.ufc.br

† geova@fisica.ufc.br

‡ wendel.mendes@ifce.edu.br

§ renan@fisica.ufc.br

alized the Ishihara method to include stationary backgrounds [33–35]. For a short review about implications of considering finite distances in the deflection of light see Ref. [36]. Currently, various papers use the Gauss-Bonnet theorem to investigate the deflection of light in black holes and wormholes [37–43]. For the Bumblebee model Casana *et al.* computed the deflection angle of light for their background [26]. However, they used the standard procedure and therefore the result is valid only for the limiting case where the distances are infinite. After this, in Ref.[44], Ovgun *et al.* found the deflection angle of light for the Casana background by using the Gibbons and Werner method. Soon later, the Ono *et al.* method was used to compute the deflection in a Kerr-like Bumblebee black hole [27]. For other applications of this methods to black hole backgrounds in Bumblebee gravity see Refs. [44–46].

However, up to now, the finite distance bending of light is missing for two of the above Bumblebee backgrounds. The first is asymptotically flat and was found by Bertolami some time ago in Ref. [25]. The second is not asymptotically flat and was found by Maluf *et al.* in Ref. [28]. This case is more interesting, since the correct bending can be obtained only by the Ishihara method of finite distance. The standard procedure does not apply to this background. Therefore, in this paper we propose

$$S_B = \int d^4x \sqrt{-g} \left[\frac{1}{2\kappa} (R - 2\Lambda + \xi R_{\mu\nu} B^\mu B^\nu) - \frac{1}{4} B_{\mu\nu} B^{\mu\nu} - V(B_\mu B^\nu \pm b^2) \right], \quad (1)$$

where $\kappa = 8\pi$, Λ is a cosmological constant, ξ is a real constant that controls the non minimal coupling between bumblebee field and curvature and b^2 is a real positive constant. The bumblebee field-strength is defined as

$$B_{\mu\nu} = D_\mu B_\nu - D_\nu B_\mu, \quad (2)$$

where D_μ is the covariant derivative. The determination of the vacuum expectation value of the bumblebee field is given when the potential is zero, $V(B^\mu B_\mu \pm b^2) = 0$. When this occurs, we have $B^\mu B_\mu \pm b^2 = 0$, and the bumblebee field vacuum expected value is b^μ , with $b^\mu b_\mu = \mp b^2$. The quantity b_μ is the coefficient of Lorentz and CTP violation, and the \pm signs in the potential dictates the nature of b_μ is timelike or spacelike. For more details in SME and Bumblebee model see [20–26, 28] and references therein. Hereafter, we will present three black hole solutions in bumblebee gravity and its characteristics. Two of these solutions [25, 26] are labeled Schwarzschild-like because do not consider a cosmological constant ($\Lambda = 0$). These solutions become the Schwarzschild solution when the vacuum expectation value of the bumblebee field is null. The other solution is Kottler-like, which arises when we take into account a nonzero cosmological constant. This black hole solution becomes the Kottler solution when the vacuum expectation value of the bum-

to apply the Ishihara method to compute the bending of light in the backgrounds of Refs. [25, 28]. The structure of the paper is as follows. In Section II, we review the Bumblebee model and the background solutions of Refs. [25, 26, 28]. In Section III, we review the Ishihara method [32], its conditions of applicability and give some examples. In Section IV, we use the Ishihara method to compute the deflection of light for the Bertolami and Páramos background, and for the Maluf and Neves background. Finally, in section V we summarize our main results.

II. BLACK HOLE SOLUTIONS IN BUMBLEBEE GRAVITY

In this section we review the Bumblebee model. It is a SME which violates the Lorentz symmetry through a vector field B_μ , called the bumblebee field. Although very simple, this model has interesting features as boost, rotation, and CPT violation. The Lorentz and diffeomorphism violation occur due to the nonvanishing vacuum expectation value of the bumblebee field [22, 23]. The action of the bumblebee model for a spacetime with a cosmological constant and null torsion is given by

blebee field is null. The Kottler solution describes matter from cosmological constant Λ around a spherical source of mass, this solution generalizes the Schwarzschild vacuum solution [47].

The solutions mentioned above share some hypotheses. First, they are static and spherically symmetric. Therefore we the ansatz for the metric is given by

$$g_{\mu\nu} = \text{diag} \left(-e^{2\gamma(r)}, e^{2\rho(r)}, r^2, r^2 \sin^2 \theta \right), \quad (3)$$

where $\gamma(r)$ and $\rho(r)$ are functions only of the radial coordinate. Second, the hypothesis that the bumblebee field B_μ remains frozen in its vacuum expectation value b_μ . Moreover, it is assumed that the vacuum expectation value of the bumblebee field b_μ is radial-like, $b_\mu = (0, b_r(r), 0, 0)$.

A. Schwarzschild-like solution

The first solution we will discuss is the one found by Bertolami and Páramos [25]. In order to find b_μ , they impose $D_\mu b_\nu = \partial_\mu b_\nu - \Gamma_{\mu\nu}^\sigma b_\sigma = 0$, what implies that

$$b_r(r) = \xi^{-1/2} b_0 e^\rho. \quad (4)$$

With this, the line element for the Bertolami and Páramos solution is given by

$$ds^2 = -f_B(r) + \frac{1}{f_B(r)}dr^2 + r^2d\Omega^2, \quad (5a)$$

where

$$f_B(r) = \left[1 - \frac{2M}{r} \left(\frac{r}{L_0} \right)^{l_B} \right] dt^2. \quad (5b)$$

In the above equations L_0 is an arbitrary distance, $l_B \approx b_0^2/2$, and $M = Gm$ is the geometrical mass[25]. In order to analyze the behavior of the solution we calculate the Ricci scalar and the Kretschmann scalar. It's easy to compute the Ricci scalar, which is

$$R_{Bertolami} = \frac{2M}{r^3} \left(\frac{r}{L_0} \right)^{l_B} (1 + l_B)l_B. \quad (6)$$

Note that, although the Bertolami solution is Schwarzschild-like, the Ricci scalar is nonzero. The Kretschmann scalar is defined by $K = R^{\mu\nu\sigma\beta}R_{\mu\nu\sigma\beta}$. In the limit $l_B \ll 0$, this scalar is

$$K_{Bertolami} = \left(1 - \frac{5}{3}l_B \right) \left(\frac{r}{L_0} \right)^{2l_B} \left(\frac{14M}{r^6} \right). \quad (7)$$

Note that both, $R_{Bertolami}$ and $K_{Bertolami}$, go to zero when $r \rightarrow \infty$, for more details see [25]. Therefore this solution is asymptotically flat.

The second solution was found by Casana *et al.* [26]. The authors do not use the condition $D_\mu b_\nu = 0$. The way used by them to determine b_μ is by the condition $b^\mu b_\mu = b^2 = const.$, and with this

$$b_r(r) = |b| e^{\rho(r)}. \quad (8)$$

So, the line element for the Casana *et al.* solution is given by

$$ds^2 = -f_c(r)dt^2 + (1 + l_c)\frac{1}{f_c(r)}dr^2 + r^2d\Omega^2, \quad (9a)$$

where

$$f_c(r) = 1 - \frac{2M}{r}. \quad (9b)$$

In the above equations $M = Gm$ is the geometric mass and $l_c = \xi b^2$. Therefore l_c depends on the vacuum expectation value of the Bumblebee field and on the coupling constant ξ . Similarly as done for the Bertolami and Páramos solution, we compute the Ricci scalar for the Casana *et al.* solution, which is

$$R_{Casana} = \frac{2}{r^2} \frac{l_c}{1 + l_c}. \quad (10)$$

As in the case of Bertolami and Páramos solution, the Casana *et al.* solution is Schwarzschild-like, but the Ricci scalar is nonzero. The Kretschmann scalar is given by

$$K_{Casana} = \frac{4(12M^2 + 4Mr l_c + l_c^2 r^2)}{r^6(1 + l_c)^2}. \quad (11)$$

Note that both solutions above have the Ricci and Kretschmann scalars go to zero in the limit of ($r \rightarrow \infty$), this fact suggests that both solutions are asymptotically flat.

B. Kottler-like solution

Now we will review a black hole solution found recently by Maluf and Neves[28]. They consider a cosmological constant in the bumblebee gravity and therefore it is not asymptotically flat. The action used to construct this solution is expressed in equation (1). However, differently from the two solutions above, the cosmological constant is nonzero. Maluf and Neves have used a linear potential

$$V(B_\mu B^\nu \pm b^2) = \frac{\lambda}{2} (B_\mu B^\nu - b^2), \quad (12)$$

where λ is a Lagrange-multiplier. Note that $V = 0$ and $V' \equiv dV(y)/dy = \lambda/2$ when $B_\mu B^\nu = b^2$. The linear potential was chosen to produce a black hole solution with a nonzero cosmological constant. With this they found the solution

$$ds^2 = -f_M(r)dt^2 + (1 + l_c)\frac{1}{f_M(r)}dr^2 + r^2d\Omega^2, \quad (13a)$$

where

$$f_M(r) = 1 - \frac{2M}{r} - (1 + l_c)\frac{\Lambda_e}{3}r^2. \quad (13b)$$

In the above equations we have that $l_c = \xi b^2$ and

$$\Lambda_e = \frac{\kappa\lambda}{\xi}. \quad (14)$$

Therefore we have an effective cosmological constant which depends on the non minimal coupling constant ξ and on the Lagrange-multiplier field λ . Just as it was done for Schwarzschild-like solutions, we will present the Ricci scalar and Kretschmann scalar. The Ricci scalar for the solution above solution is given by

$$R_{Maluf} = 4\Lambda_e + \frac{2}{r^2} \frac{l_c}{1 + l_c}, \quad (15)$$

and the Kretschmann scalar is

$$K_{Maluf} = \frac{8}{3}\Lambda_e^2 + \frac{l_c}{(1 + l_c)r^2} \left[\frac{8}{3}\Lambda_e + \frac{4l_c}{(1 + l_c)r^2} + \frac{16M}{(1 + l_c)r^3} + \frac{48M^2}{l_c(1 + l_c)r^4} \right]. \quad (16)$$

The Ricci's and Kretschmann scalars for the above Kottler-like solution go, respectively, to $4\Lambda_e$ and $8\Lambda_e^2/3$ when $r \rightarrow \infty$. As expected, the effective cosmological constant provides a constant curvature at the same limit. Then, as we will see, the correct method to compute the deflection angle of light is the one proposed by Ishihara.

III. BENDING ANGLE OF LIGHT FOR FINITE DISTANCES AND GAUSS-BONNET THEOREM

In this section we review the Ishihara method and the conditions of validity for this approach[32]. It is a way to determine the bending angle of light by gravity in a

static and spherically symmetrical spacetime. This approach examines the connection between the bending angle of light and the Gauss-Bonnet theorem through the optical metric. Moreover, it allows the computation of the deflection angle of light for non asymptotically flat spacetimes because, since it considers the finite distances between the observer, lens, and source.

A class of solutions of the gravity field equations is obtained when the source has spherical symmetry. Although simple, this class of solutions is very useful. Here, we consider a subclass which refers to static and spherically symmetric metric, which can be represented by

$$ds^2 = -A(r)dt^2 + B(r)dr^2 + r^2d\Omega^2. \quad (17)$$

In the above equation $d\Omega^2 = d\theta^2 + \sin^2\theta d\phi^2$ is the solid angle, and the coefficients $A(r)$ and $B(r)$ are independent of time [3, 5]. We focus on trajectories of light rays, which obey the null condition ($ds^2 = 0$). These trajectories can be described by means of geodesics of the optical metric due to the generalization of Fermat's principle [5]. The optical metric defines a three-dimensional Riemann space in which the light ray is expressed as a spatial curve. Without loss of generality we can consider $\theta = \pi/2$ and the optical metric for obtained from (17) is given by

$$dt^2 = \frac{B(r)}{A(r)}dr^2 + \frac{r^2}{A(r)}d\phi^2. \quad (18)$$

Furthermore, using the coordinate transformation $u = 1/r$ and the impact parameter $b = [r^2/A(r)]d\phi/dt$, the orbit equation can be derived from optical metric and is give by

$$\left(\frac{du}{d\phi}\right)^2 = F(u) = \frac{1}{b^2AB} - \frac{u^2}{B}, \quad (19)$$

where $A = A(1/u)$ and $B = B(1/u)$.

The usual approach to calculate the deflection angle of light is to study the orbit equation assuming the weak deflection limit. This method was used by Casana *et al.* in Ref. [26]. Let's reproduce their result here in order to exemplify this approach. By using the Casana's background, Eq.(9a) and Eq.(9b), the above orbit equation (19) becomes

$$(1 + l_c) \left(\frac{du}{d\phi}\right)^2 = \frac{1}{b^2} - u^2 + 2Mu^3. \quad (20)$$

If we differentiate equation (20) above with respect to ϕ , we find

$$(1 + l_c) \frac{d^2u}{d\phi^2} + u - 3Mu^2 = 0. \quad (21)$$

The weak deflection limit consists of considering the quantity Mu as sufficiently small. In this way, we can use a perturbative method to calculate u up to the first order in Mu . By using the ansatz $u = u^{(0)} + 3Mu^{(1)}$, we

find

$$u = \frac{1}{b} \sin\left(\frac{\phi}{\sqrt{1+l_c}}\right) + \frac{M}{b^2} \left[1 + A \cos\left(\frac{\phi}{\sqrt{1+l_c}}\right) + \cos^2\left(\frac{\phi}{\sqrt{1+l_c}}\right)\right], \quad (22)$$

where A is an arbitrary constant. The boundary conditions used by Casana *et al.* to find the deflection angle of light are: the source is located at $u = 0$ ($r \rightarrow \infty$) with $\phi = -\delta_1$ and the observer is located at $u = 0$ ($r \rightarrow \infty$) with $\phi = \delta_2$. The deflection angle of light is $\alpha = \delta_1 + \delta_2$. Taking into consideration that $\delta_1 \ll 1$, $\delta_2 \ll 1$, and $l_c \ll 1$, we can find the deflection angle of light in first-order as

$$\alpha = \frac{4M}{b} + \frac{\pi l_c}{2}. \quad (23)$$

We should point that we need to use just the orbit equation and the weak deflection limit to find the deflection angle of light. Below we present two new methods, which are based on the Gauss-bonnet theorem, to compute this deflection: the Gibbons and Werner method and the Ishihara method.

The Gauss-Bonnet theorem is an elegant result that associates the geometrical characteristics of a two-dimensional surface with its topological Euler characteristic. Let the domain (D, χ, g) be a subset of a compact, oriented surface, with Euler characteristic χ and a Riemann metric g giving rise to a Gaussian curvature K . Moreover, let $\partial D : \{t\} \rightarrow D$ be a piecewise smooth boundary with geodesic curvature κ , and θ_i the external angle at i th vertex, traversed in the positive sense (see figure 1). Then the Gauss-Bonnet theorem can be stated by

$$\int \int_D K dS + \int_{\partial D} \kappa dt + \sum_i \theta_i = 2\pi\chi(D). \quad (24)$$

For more details about the Gauss-Bonnet theorem and its applications see Refs.[29, 30]. Observe that the Gauss-Bonnet theorem can be used only on a two-dimensional surface, but spacetime has four dimensions.

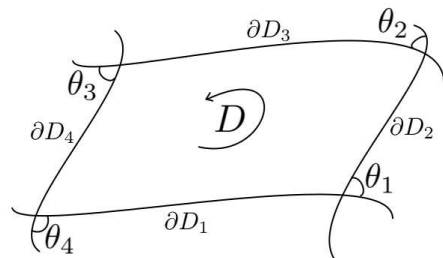


FIG. 1. Schematic figure for the Gauss-Bonnet theorem.

The Gibbons and Werner method uses the Gauss-Bonnet theorem in the space of optical metric to compute the deflection angle of light. They have found that

this deflection is given by

$$\int_0^{\pi+\alpha} \kappa \frac{dt}{d\phi} d\phi - \pi = - \int \int_D K dS, \quad (25)$$

where α is the deflection angle of light, κ is the geodesic curvature of the circular sector centered on the lens, K is the Gaussian curvature of the optical metric, and dS is the area element of the surface. The domain D is the surface between the null geodesic from the source to receiver and the circular sector centered on the lens. By using the Gibbons and Werner method, Ovgun *et al.* find the deflection angle of light for the Casana *et al.* background [44]. The result found by Ovgun *et al.* is the same as equation (23) in first order.

Now, we present the Ishihara method. For that, we define the unit tangential vector along of the light ray,

$$(V^r, V^\varphi) = \frac{bA(r)}{r^2} \left(\frac{dr}{d\varphi}, 1 \right), \quad (26)$$

and the unit vectors along the radial direction from the center of the lens $e_{rad} = (\sqrt{A/B}, 0)$ and along the angular direction $e_{ang} = (0, \sqrt{A/r^2})$. Note that the optical metric of the equation (18) defines a two-dimensional surface, and it is in this space that the Gauss-Bonnet theorem is applied. The application of the Gauss-Bonnet theorem is realized in the optical metric for the system Receiver-Lens-Source, see figure 2(taken from [32]).

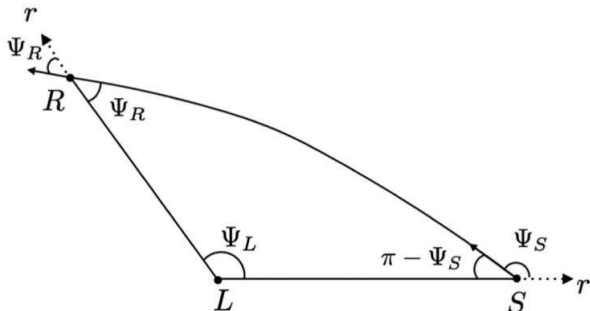


FIG. 2. Schematic figure for the Receiver-Lens-Source system [32].

According to these definitions, Ishihara arrives at the deflection angle of light, which is given by

$$\alpha = \Psi_R - \Psi_S + \int_{u_R}^{u_0} \frac{du}{\sqrt{F(u)}} + \int_{u_S}^{u_0} \frac{du}{\sqrt{F(u)}}, \quad (27)$$

where u_R is the inverse of the distance between the lens and receiver, u_S is the inverse of the distance between the lens and source, and r_0 is the inverse of the closest trajectory point of the lens. The angle Ψ indicates the angle of the light ray measured from the radial direction at a trajectory point(see figure 1). This angle, at radial position r can be expressed by

$$\Psi(u) = \arcsin \left(bu \sqrt{A(r)} \right), \quad (28)$$

where $u = 1/r$. The quantity $\Psi_R - \Psi_S$ can be expressed in terms of the inverse sine function,

$$\begin{aligned} \Psi_R - \Psi_S = & \arcsin \left(bu_R \sqrt{A(r_R)} \right) \\ & + \arcsin \left(bu_S \sqrt{A(r_S)} \right) - \pi. \end{aligned} \quad (29)$$

In the limit $(r_R, r_S) \rightarrow (\infty, \infty)$, the deflection angle of light (27) becomes

$$\alpha_0 = 2 \int_0^{u_0} \frac{du}{\sqrt{F(u)}} - \pi. \quad (30)$$

As an example of the Ishihara method, we apply it to the Casana *et al.* background given in Eq.(9a). This deflection angle of light for this background has yet not been found by the direct use of this method. However, Ovgun *et al.* has found the bending of light for a rotating Bumblebee black hole[27]. By taking the limit of null rotation and infinite distance of this Kerr-like deflection, we can recover the result found by Casana. However, Ovgun *et al.* did not use the Ishihara method. Here we will obtain the finite distance deflection directly from the Ishihara method. We begin by considering the equations (9a) and (9b) to build the term $\Psi_R - \Psi_S$ and by using the weak deflection limit ($2M/b \ll 1$). So, we get

$$\begin{aligned} \Psi_R - \Psi_S = & \arcsin(bu_R) + \arcsin(bu_S) - \pi \\ & - \frac{1}{2} \frac{2M}{b} \left[\frac{b^2 u_R^2}{\sqrt{1 - b^2 u_R^2}} + \frac{b^2 u_S^2}{\sqrt{1 - b^2 u_S^2}} \right] \\ & + O \left(\frac{4M^2}{b^2} \right). \end{aligned} \quad (31)$$

To find the deflection angle of light, we compute the integrations present in equation (27). These integrations can be simplified by the use of the second fundamental theorem of calculus and becomes

$$\int_u^{u_0} \frac{du'}{\sqrt{F(u')}} = I(u_0) - I(u), \quad (32)$$

where $I(u)$ is the antiderivative of $F(u)^{-1/2}$. The orbit equation (19) for the Casana *et al.* background then becomes

$$F(u) = (1 + l_c)^{-1} \left[\frac{1}{b^2} - u^2 + bu^3 \frac{2M}{b} \right]. \quad (33)$$

Now, expanding $F(u)^{-1/2}$ and computing its antiderivative, we obtain

$$\begin{aligned} I(u) = & \sqrt{1 + l_c} \left[\arcsin(bu) - \frac{M}{b} \frac{2 - (bu)^2}{\sqrt{1 - (bu)^2}} \right] \\ & + O \left(\frac{4M^2}{b^2} \right). \end{aligned} \quad (34)$$

Finally, by using the equations (31) and (34) in (27), the deflection angle of light can be written as

$$\alpha = 2I(u_0) - \pi - (\lambda - 1) [\arcsin(bu_R) + \arcsin(bu_S)] + \frac{M}{b} \left[\frac{2\lambda - (bu_R)^2(\lambda + 1)}{\sqrt{1 - (bu_R)^2}} + \frac{2\lambda - (bu_S)^2(\lambda + 1)}{\sqrt{1 - (bu_S)^2}} \right], \quad (35)$$

where $\lambda = \sqrt{1 + l_c}$. Let's now find the value $I(u_0)$. We can do this through the limit $bu_R \approx bu_S \approx 0$ and by observing that $I(u_0) = \lambda I^{Sch}(u_0)$, where $I^{Sch}(u_0)$ is the antiderivative of $F(u)^{-1/2}$ for Schwarzschild background. We know that the deflection angle of light for the Schwarzschild background, disregarding finite distances, is $4M/b$. Note also that the equation (35) for both limit $l_c = 0$ and $bu_R \approx bu_S \approx 0$ becomes the deflection angle of light for the Schwarzschild case. Therefore we can see that

$$\frac{4M}{b} = 2I^{Sch}(u_0) - \pi + \frac{4M}{b} + O\left(\frac{4M^2}{b^2}\right), \quad (36)$$

and we can conclude that $2I(u_0) = \lambda\pi$. The bending angle of light for the Casana *et al.* background, considering finite distances, is finally given by

$$\alpha = (\lambda - 1) [\pi - \arcsin(bu_R) - \arcsin(bu_S)] + \left[\frac{2\lambda - (bu_R)^2(1 + \lambda)}{\sqrt{1 - (bu_R)^2}} + \frac{2\lambda - (bu_S)^2(1 + \lambda)}{\sqrt{1 - (bu_S)^2}} \right] \frac{M}{b}, \quad (37)$$

We should point that the above has never been obtained by the straight use of the Ishihara method. Casana *et al.* has found it by using the standard procedure. Later, Ovgun *et al.* found it by using the Gibbons and Werner method [44]. It can also be obtained by performing the limit of null rotation of the Kerr-like black hole in bumblebee gravity [27]. Therefore, despite of using this new method, we keep this result as an example of the Ishihara method. Now, we will analyze the deflection angle of light, equation (37), in the three limit cases as follows.

First, note that for the limit of the bumblebee field having a null vacuum expectation value ($l_c = 0$) and disregarding finite distances ($bu_R \approx bu_S \approx 0$), the equation (37) becomes the Schwarzschild deflection angle,

$$\alpha = \frac{4M}{b}. \quad (38)$$

This was expected since when $l_c = 0$ the Casana *et al.* background becomes Schwarzschild background. Second, disregarding just finite distances and consider $l_c \ll 1$ the equation (37) becomes equation (23). That is, this result agrees with the result presented by Casana *et al.* [26] and in the first order with the paper [44] that uses Gibbons and Werner method [31]. Finally, considering the case that both the receiver and the source are very far from the lens and the trajectory light ray passes far from the

lens ($u_R \approx bu_S \approx 1$), the equation (37) produces the null deflection of light $\alpha = 0$ (see figure 3). This null deflection angle agrees with the fact that in the limit $r \rightarrow \infty$ both Ricci and Kretschmann scalars tend to zero.

The importance to consider finite distances is in the fact that only with this consideration was it possible to study the regimes expressed in the three cases above. In the next section, we analyze the deflection angle of light for the Bertolami and Páramos background, and the Maluf and Neves background.

IV. BENDING ANGLE OF LIGHT FOR BLACK HOLE SOLUTION IN BUMBLEBEE GRAVITY

This section is designated to computer the deflection angle of light using the Ishihara method presented in section III. This is done for the Bertolami and Paramos background, and Maluf and Neves backgrounds, present in section II. We investigate the influence of the bumblebee field considering finite distances of the Receiver-Lens-Source system.

A. Bertolami's Schwarzschild-like background

In section II, we presented the Schwarzschild-like metric constructed by Bertolami and Páramos [25]. Now, we use this background, equations (5a) and (5b), to investigate the influence of bumblebee field in bending of light via Eq. (27). By using of Eq. (28), we can write

$$\Psi(u) = \arcsin \left[bu \sqrt{1 - \frac{2M}{b} \frac{bu}{(uL_0)^{l_B}}} \right]. \quad (39)$$

Taking into account the limit of weak deflection $2M/b \ll 1$, we can expand the equation (39) in terms of $2M/b$ as

$$\Psi(u) = \arcsin(bu) - \frac{1}{2} \frac{2M}{b} \left(\frac{b}{L_0} \right)^{l_B} \frac{(bu)^{2-l_B}}{\sqrt{1 - (bu)^2}} + O\left(\frac{4M^2}{b^2}\right). \quad (40)$$

The bumblebee field should have a weak effect because the vacuum expectation value of this field is of order 10^{-11} [25, 26], then $l_B \ll 1$. In this way, by using $(bu)^{2-l_B} \approx (bu)^2 - l_B \ln(bu)$ we can rewrite the equation (40) as

$$\Psi(u) = \arcsin(bu) - \frac{1}{2} \frac{2M}{b} \left(\frac{b}{L_0} \right)^{l_B} \frac{(bu)^2}{\sqrt{1 - (bu)^2}} + O\left(\frac{4M^2}{b^2}, \frac{2M}{b} l_B, l_B^2\right). \quad (41)$$

With this, the $\Psi_R - \Psi_S$ contribution to the deflection angle becomes

$$\begin{aligned} \Psi_R - \Psi_S = & \arcsin(bu_R) + \arcsin(bu_S) - \pi \\ & - \frac{1}{2} \frac{2M}{b} \left(\frac{b}{L_0} \right)^{l_B} \left[\frac{(bu_R)^2}{\sqrt{1-b^2u_R^2}} + \frac{(bu_S)^2}{\sqrt{1-b^2u_S^2}} \right] \\ & + O\left(\frac{4M^2}{b^2}, \frac{2M}{b} l_B, l_B^2\right). \end{aligned} \quad (42)$$

The orbit equation (19) for the Bertolami and Páramos background provide

$$F(u) = \frac{1}{b^2} - u^2 \left(1 - \frac{2M}{b} \frac{bu}{(uL_0)^{l_B}} \right). \quad (43)$$

As done in the last section, the procedure is to expand $F(u)^{-1/2}$, realize the integrations and use the null integration constant. With this we arrive at

$$\begin{aligned} I(u) = & \arcsin(bu) - \frac{1}{2} \frac{2M}{b} \left(\frac{b}{L_0} \right)^{l_B} \frac{(2-(bu)^2)}{\sqrt{1-(bu)^2}} \\ & + O\left(\frac{2M^2}{b^2}, \frac{l_B 2M}{b}, l_B^2\right). \end{aligned} \quad (44)$$

Now we remember that in the limit $b \rightarrow 0$ the Bertolami and Páramos background recovers the Schwarzschild one. By using this we see that $I(u_0) = \pi/2$. Finally we arrive at the deflection angle of light considering finite distances for the background of Bertolami and Páramos, which is given by

$$\alpha = \frac{2M}{b} \left(\frac{b}{L_0} \right)^{l_B} \left[\sqrt{1-b^2u_R^2} + \sqrt{1-b^2u_S^2} \right]. \quad (45)$$

Let us now analyze the limiting cases. When both, the receiver and the source, are very far from the lens, but the trajectory light ray passes close to the lens, $bu_R \approx bu_S \approx 0$, the deflection angle of light becomes

$$\alpha = \frac{4M}{b} \left(\frac{b}{L_0} \right)^{l_B}. \quad (46)$$

The above result, as expected, becomes the Schwarzschild deflection angle when $l_B \rightarrow 0$. In the case that both the receiver and the source are very far from the lens and the light ray trajectory passes far from the lens, $u_R \approx bu_S \approx 1$, the deflection angle of light is null (see figure 3). This result agrees with the fact both the Ricci and Kretschmann scalars tend to zero in the background of Bertolami and Páramos [25].

B. Maluf's Kottler-like background

In this subsection, we find the deflection angle of light considering finite distances for the Maluf and Neves background and investigates the three limit cases. The procedure is the same as the one employed in last subsection. To compute $\Psi_R - \Psi_S$ we use the background, given in

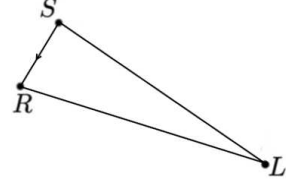


FIG. 3. Receiver-Lens-Source system with the light ray trajectory passing far from the lens.

equations (13a) and (13b), in equation (29). By defining $\sqrt{1+l_c} = \lambda$, and expanding the result in the first order of $2M/b$ and $\lambda^2 \Lambda_e$, we find

$$\begin{aligned} \Psi_R - \Psi_S = & \arcsin(bu_R) + \arcsin(bu_S) - \pi \\ & - \frac{M}{b} \left[\frac{b^2u_R^2}{\sqrt{1-b^2u_R^2}} + \frac{b^2u_S^2}{\sqrt{1-b^2u_S^2}} \right] \\ & - \frac{\lambda^2 \Lambda_e b^2}{6} \left[\frac{1}{bu_R \sqrt{1-b^2u_R^2}} + \frac{1}{bu_S \sqrt{1-b^2u_S^2}} \right] \\ & + \frac{\lambda^2 \Lambda_e M b}{6} \left[\frac{2b^2u_R^2 - 1}{(1-b^2u_R^2)^{3/2}} + \frac{2b^2u_S^2 - 1}{(1-b^2u_S^2)^{3/2}} \right] \\ & + O\left(\frac{4M^2}{b^2}, (\lambda^2 \Lambda_e)^2\right). \end{aligned} \quad (47)$$

The orbit equation (19) for the Maluf and Neves background provides

$$F(u) = \frac{1}{\lambda^2} \left[\frac{1}{b^2} - u^2 \left(1 - 2Mu - \lambda^2 \frac{\Lambda_e}{3} \frac{1}{u^2} \right) \right]. \quad (48)$$

Then, we can compute the antiderivative of $F(u)^{-1/2}$ in orders of M/b , $\lambda^2 \Lambda_e$. This is given by

$$\begin{aligned} I(u) = & \lambda \left[\arcsin(bu) - \frac{M(2-b^2u^2)}{b \sqrt{1-b^2u^2}} \right. \\ & \left. - \frac{b^2 \lambda^2 \Lambda_e}{6} \frac{ub}{\sqrt{1-b^2u^2}} + \frac{bM \lambda^2 \Lambda_e}{6} \frac{3b^2u^2 - 2}{(1-b^2u^2)^{3/2}} \right] \\ & + O\left(\frac{4M^2}{b^2}, \lambda^2 \Lambda_e^2\right). \end{aligned} \quad (49)$$

Now, we can express the bending angle of light as a function of $I(u_0)$,

$$\begin{aligned} \alpha = & 2I(u_0) - \pi - (\lambda - 1) [\arcsin(bu_R) + \arcsin(bu_S)] \\ & + \frac{M}{b} \left[\frac{2\lambda - (bu_R)^2(\lambda + 1)}{\sqrt{1-(bu_R)^2}} + \frac{2\lambda - (bu_S)^2(\lambda + 1)}{\sqrt{1-(bu_S)^2}} \right] \\ & - \frac{\lambda^2 \Lambda_e b^2}{6} \left[\frac{1 - \lambda b^2 u_R^2}{bu_R \sqrt{1-b^2u_R^2}} + \frac{1 - \lambda b^2 u_S^2}{bu_S \sqrt{1-b^2u_S^2}} \right] \\ & + \frac{\lambda^2 \Lambda_e M b}{6} \left[\frac{2\lambda - 1 + (2-3\lambda)b^2u_R^2}{(1-b^2u_R^2)^{3/2}} + \right. \\ & \left. + \frac{2\lambda - 1 + (2-3\lambda)b^2u_S^2}{(1-b^2u_S^2)^{3/2}} \right] + O\left(\frac{4M^2}{b^2}, \lambda^2 \Lambda_e^2\right). \end{aligned} \quad (50)$$

Note that if the cosmological constant is null, then the angle of deflection of light must become the Casana one, given in equation (37). With this we deduce that $2I(u_0) = \lambda\pi$. Finally we arrive at the deflection angle, considering finite distances, for the Maluf and Neves background. It is given by

$$\begin{aligned} \alpha = & (\lambda - 1) [\pi - \arcsin(bu_R) - \arcsin(bu_S)] \\ & + \frac{M}{b} \left[\frac{2\lambda - (bu_R)^2(\lambda + 1)}{\sqrt{1 - (bu_R)^2}} + \frac{2\lambda - (bu_S)^2(\lambda + 1)}{\sqrt{1 - (bu_S)^2}} \right] \\ & - \frac{\lambda^2 \Lambda_e b^2}{6} \left[\frac{1 - \lambda b^2 u_R^2}{bu_R \sqrt{1 - b^2 u_R^2}} + \frac{1 - \lambda b^2 u_S^2}{bu_S \sqrt{1 - b^2 u_S^2}} \right] \\ & + \frac{\lambda^2 \Lambda_e M b}{6} \left[\frac{2\lambda - 1 + (2 - 3\lambda)b^2 u_R^2}{(1 - b^2 u_R^2)^{3/2}} + \right. \\ & \left. + \frac{2\lambda - 1 + (2 - 3\lambda)b^2 u_S^2}{(1 - b^2 u_S^2)^{3/2}} \right] + O\left(\frac{4M^2}{b^2}, \lambda^2 \Lambda_e^2\right). \end{aligned} \quad (51)$$

Let's now investigate the three limiting cases. First, if the bumblebee field null, then the deflection angle of light becomes the deflection angle for the Kottler background presented by Ishihara *et al.* [32]. Second, if we disregard finite distances ($bu_R \approx bu_S \approx 0$) and considers $l_c \ll 1$, the bending angle of light becomes

$$\alpha = \frac{4M}{b} - \frac{b^2 \Lambda_e}{6} \left[\frac{1}{bu_R} + \frac{1}{bu_S} \right] + \frac{bM\Lambda_e}{3} + \frac{\pi l_c}{2}. \quad (52)$$

Although some terms apparently diverge, this limit is not relevant for astronomical observations [32]. Finally, we can consider that the receiver and the source are very far from the lens and the light ray trajectory passes far from the lens ($bu_R \approx bu_S \approx 1$) and $l_c \ll 1$. In this limit, the deflection angle of light becomes

$$\alpha = \frac{bM\lambda^2 \Lambda_e}{6} \left[\frac{1}{\sqrt{1 - b^2 u_R^2}} + \frac{1}{\sqrt{1 - b^2 u_S^2}} \right]. \quad (53)$$

Again, although the equation (53) apparently diverges, all objects that compose the Receiver-Lens-Source system are at a finite distance from the other, thus this divergence does not matter.

V. CONCLUSION

In this paper, we computed the deflection angle of light for black hole backgrounds in bumblebee gravity. For this we use the Ishihara method, which can be used in non asymptotically flat spacetimes. Moreover, we analyze the influence of the bumblebee field on this deflection. We consider three backgrounds. Two of them are asymptotically flat: i) the one found by Casana *et al.* in reference [26], ii) the one found by Bertolami *et al.* in Ref. [25]. The last one has an effective cosmological constant and therefore is not asymptotically flat: iii) the one found by

Maluf *et al.* in Ref. [28]. We also investigated the three limiting cases: a) a null vacuum expectation value for the bumblebee field, b) that both the receiver and the source are very far from the lens, but the trajectory light ray passes close to the lens and c) that both the receiver and the source are very far from the lens and the trajectory light ray passes far from the lens.

Let us begin by considering case i). The deflection angle for the Casana *et al.* background has never been obtained with the Ishihara method. However, it has been found in two different ways: in Ref. [44] by using the Gibbons *et al.* method and in Ref. [27] by using the Ono method. Therefore, the result with the Ishihara method was presented in Eq. (37) of review section III and is given by

$$\begin{aligned} \alpha = & (\lambda - 1) [\pi - \arcsin(bu_R) - \arcsin(bu_S)] \\ & + \left[\frac{2\lambda - (bu_R)^2(1 + \lambda)}{\sqrt{1 - (bu_R)^2}} + \frac{2\lambda - (bu_S)^2(1 + \lambda)}{\sqrt{1 - (bu_S)^2}} \right] \frac{M}{b}. \end{aligned} \quad (54)$$

The above expression can be obtained by considering the null rotation in the result found by Ono *et al.* in Ref. [27]. In order to recover the result found by Casana we must analyze the correct limits. For the limiting case a) the deflection angle of light are the same as in the Schwarzschild case. When considering the limiting case b), we found in (23) that

$$\alpha = \frac{4M}{b} + \frac{\pi l_c}{2},$$

which is the result of Casana *et al.*. When considering the limiting case c), we conclude that the deflection angle of light in this limit is null.

Now let us consider the case ii). We have found the deflection angle of light for the Bertolami and Páramos background, considering finite distances, in equation (45)

$$\alpha = \frac{2M}{b} \left(\frac{b}{L_0} \right)^{l_B} \left[\sqrt{1 - b^2 u_R^2} + \sqrt{1 - b^2 u_S^2} \right].$$

We can see that the influence of the bumblebee field is just a multiplicative term $(b/L_0)^{l_B}$. For the limiting case a) the deflection angle of light are the same as in the Schwarzschild case. The limiting case b) was given in Eq. (46) and is given by

$$\alpha = \frac{4M}{b} \left(\frac{b}{L_0} \right)^{l_B}.$$

When considering the limiting case c), we conclude that the deflection angle of light in this limit is null.

Finally, we consider the case iii), the Maluf and Neves background, which is not asymptotically flat. Moreover, the cosmological constant depends on the characteristics of the bumblebee field interaction, according to the equation (14). The deflection angle of light, considering finite

distances, for this background was presented in equation (51) and is given by

$$\begin{aligned} \alpha = & (\lambda - 1) [\pi - \arcsin(bu_R) - \arcsin(bu_S)] \\ & + \frac{M}{b} \left[\frac{2\lambda - (bu_R)^2(\lambda + 1)}{\sqrt{1 - (bu_R)^2}} + \frac{2\lambda - (bu_S)^2(\lambda + 1)}{\sqrt{1 - (bu_S)^2}} \right] \\ & - \frac{\lambda^2 \Lambda_e b^2}{6} \left[\frac{1 - \lambda b^2 u_R^2}{bu_R \sqrt{1 - b^2 u_R^2}} + \frac{1 - \lambda b^2 u_S^2}{bu_S \sqrt{1 - b^2 u_S^2}} \right] \\ & + \frac{\lambda^2 \Lambda_e M b}{6} \left[\frac{2\lambda - 1 + (2 - 3\lambda)b^2 u_R^2}{(1 - b^2 u_R^2)^{3/2}} + \right. \\ & \left. + \frac{2\lambda - 1 + (2 - 3\lambda)b^2 u_S^2}{(1 - b^2 u_S^2)^{3/2}} \right] + O\left(\frac{4M^2}{b^2}, \lambda^2 \Lambda_e^2\right). \end{aligned}$$

This result show that the influence of the bumblebee field in the deflection angle of light is through the parameter $\lambda = \sqrt{1 + l_c}$. We studied the three limiting cases for this deflection angle. For the case a) , we found that the deflection angle recovers the Kottler result presented in [32]. For the case b), we found that the deflection angle of light becomes expressed by equation (52),

$$\alpha = \frac{4M}{b} - \frac{b^2 \Lambda_e}{6} \left[\frac{1}{bu_R} + \frac{1}{bu_S} \right] + \frac{bM\Lambda_e}{3} + \frac{\pi l_c}{2}.$$

Finally, when we considered the limiting case c), we found

that the deflection angle of light became expressed by equation (53),

$$\alpha = \frac{bM\lambda^2 \Lambda_e}{6} \left[\frac{1}{\sqrt{1 - b^2 u_R^2}} + \frac{1}{\sqrt{1 - b^2 u_S^2}} \right].$$

The apparent divergences that arise do not matter, because the constituents of the Receiver-Lens-Source system have finite distances from each other.

We should point that the two asymptotically flat backgrounds above share some properties. For the limiting case a) both the deflection angles of light are the same as in the Schwarzschild case. This is expected since, as shown in sec II, in the limit $b \rightarrow 0$ both Schwarzschild-like black holes must recover the Schwarzschild one. For the limiting case b) the deflection angles are null for both backgrounds. This result is consistent with the fact that both Ricci and Kretschmann scalars go to zero in the limit $r \rightarrow \infty$ in both cases. Finally, in the near future, we intend to study the deflection of massive particles by using the Ishihara method.

ACKNOWLEDGMENTS

We thanks Coordenação de Aperfeiçoamento de Pessoal de Nível Superior (CAPES), and Conselho Nacional de Desenvolvimento Científico e Tecnológico (CNPq) for the financial support.

-
- [1] N. Doughty, *Lagrangian interaction: an introduction to relativistic symmetry in electrodynamics and gravitation* (CRC Press, 2018).
- [2] F. W. Dyson, A. S. Eddington, and C. Davidson, A determination of the deflection of light by the sun's gravitational field, from observations made at the total eclipse of may 29, 1919, *Philosophical Transactions of the Royal Society of London. Series A, Containing Papers of a Mathematical or Physical Character* **220**, 291 (1920).
- [3] S. Weinberg, *Gravitation and cosmology*, Vol. 67 (Wiley, New York, 1972).
- [4] L. D. Landau, *The classical theory of fields* (Elsevier, v. 2, 2013).
- [5] T. Padmanabhan, *Gravitation* (Cambridge University Press, 2010).
- [6] C. W. Misner, K. S. Thorne, J. A. Wheeler, *et al.*, *Gravitation* (Macmillan, 1973).
- [7] B. Abbott *et al.* (LIGO Scientific, Virgo), Observation of Gravitational Waves from a Binary Black Hole Merger, *Phys. Rev. Lett.* **116**, 061102 (2016), arXiv:1602.03837 [gr-qc].
- [8] K. Akiyama *et al.* (Event Horizon Telescope), First M87 Event Horizon Telescope Results. I. The Shadow of the Supermassive Black Hole, *Astrophys. J.* **875**, L1 (2019), arXiv:1906.11238 [astro-ph.GA].
- [9] P. Schneider, J. Ehlers, and E. Falco, *Gravitational Lenses* (Springer, 1992).
- [10] J. Wambsganss, Gravitational lensing in astronomy, *Living Rev. Rel.* **1**, 12 (1998), arXiv:astro-ph/9812021.
- [11] M. Bartelmann, Gravitational lensing, *Classical and Quantum Gravity* **27**, 233001 (2010).
- [12] N. Inada, M. Oguri, M.-S. Shin, I. Kayo, M. A. Strauss, T. Morokuma, C. E. Rusu, M. Fukugita, C. S. Kochanek, G. T. Richards, *et al.*, The sloan digital sky survey quasar lens search. v. final catalog from the seventh data release, *The Astronomical Journal* **143**, 119 (2012).
- [13] S. Suyu, M. Auger, S. Hilbert, P. Marshall, M. Tewes, T. Treu, C. Fassnacht, L. Koopmans, D. Sluse, R. Blandford, *et al.*, Two accurate time-delay distances from strong lensing: Implications for cosmology, *The Astrophysical Journal* **766**, 70 (2013).
- [14] T. E. Collett and M. W. Auger, Cosmological Constraints from the double source plane lens SDSSJ0946+1006, *Mon. Not. Roy. Astron. Soc.* **443**, 969 (2014), arXiv:1403.5278 [astro-ph.CO].
- [15] J.-P. Beaulieu *et al.* (MOA), Discovery of a cool planet of 5.5 earth masses through gravitational microlensing, *Nature* **439**, 437 (2006), arXiv:astro-ph/0601563.
- [16] B. Gaudi, D. Bennett, A. Udalski, A. Gould, G. Christie, D. Maoz, S. Dong, J. McCormick, M. Szymański, P. Tristram, *et al.*, Discovery of a jupiter/saturn analog with gravitational microlensing, *Science* **319**, 927 (2008).
- [17] C. Alcock *et al.* (MACHO), The MACHO project: Microlensing results from 5.7 years of LMC observations, *Astrophys. J.* **542**, 281 (2000), arXiv:astro-ph/0001272.
- [18] L. Morel, Z. Yao, P. Cladé, and S. Guellati-Khélifa, De-

- termination of the fine-structure constant with an accuracy of 81 parts per trillion, *Nature* **588**, 61 (2020).
- [19] S. Weinberg, The Making of the standard model, *Eur. Phys. J. C* **34**, 5 (2004), arXiv:hep-ph/0401010.
- [20] D. Colladay and V. A. Kostelecký, Cpt violation and the standard model, *Physical Review D* **55**, 6760 (1997).
- [21] D. Colladay and V. A. Kostelecký, Lorentz violating extension of the standard model, *Phys. Rev. D* **58**, 116002 (1998), arXiv:hep-ph/9809521.
- [22] V. A. Kostelecký, Gravity, Lorentz violation, and the standard model, *Phys. Rev. D* **69**, 105009 (2004), arXiv:hep-th/0312310.
- [23] R. Bluhm and V. A. Kostelecký, Spontaneous Lorentz violation, Nambu-Goldstone modes, and gravity, *Phys. Rev. D* **71**, 065008 (2005), arXiv:hep-th/0412320.
- [24] R. Bluhm, S.-H. Fung, and V. A. Kostelecký, Spontaneous lorentz and diffeomorphism violation, massive modes, and gravity, *Physical Review D* **77**, 065020 (2008).
- [25] O. Bertolami and J. Paramos, Vacuum solutions of a gravity model with vector-induced spontaneous lorentz symmetry breaking, *Physical Review D* **72**, 044001 (2005).
- [26] R. Casana, A. Cavalcante, F. Poulis, and E. Santos, Exact schwarzschild-like solution in a bumblebee gravity model, *Physical Review D* **97**, 104001 (2018).
- [27] Z. Li and A. Övgün, Finite-distance gravitational deflection of massive particles by a Kerr-like black hole in the bumblebee gravity model, *Phys. Rev. D* **101**, 024040 (2020), arXiv:2001.02074 [gr-qc].
- [28] R. V. Maluf and J. C. S. Neves, Black holes with a cosmological constant in the bumblebee gravity, *Physical Review D* (2020), arXiv:2011.12841 [gr-qc].
- [29] M. P. Do Carmo, *Differential geometry of curves and surfaces: revised and updated second edition* (Courier Dover Publications, 2016).
- [30] W. Klingenberg, *A course in differential geometry*, Vol. 51 (Springer Science & Business Media, 2013).
- [31] G. Gibbons and M. Werner, Applications of the gauss-bonnet theorem to gravitational lensing, *Classical and Quantum Gravity* **25**, 235009 (2008).
- [32] A. Ishihara, Y. Suzuki, T. Ono, T. Kitamura, and H. Asada, Gravitational bending angle of light for finite distance and the gauss-bonnet theorem, *Physical Review D* **94**, 084015 (2016).
- [33] T. Ono, A. Ishihara, and H. Asada, Gravitomagnetic bending angle of light with finite-distance corrections in stationary axisymmetric spacetimes, *Physical Review D* **96**, 104037 (2017).
- [34] T. Ono, A. Ishihara, and H. Asada, Deflection angle of light for an observer and source at finite distance from a rotating wormhole, *Physical Review D* **98**, 044047 (2018).
- [35] T. Ono, A. Ishihara, and H. Asada, Deflection angle of light for an observer and source at finite distance from a rotating global monopole, *Physical Review D* **99**, 124030 (2019).
- [36] T. Ono and H. Asada, The effects of finite distance on the gravitational deflection angle of light, *Universe* **5**, 218 (2019), arXiv:1906.02414 [gr-qc].
- [37] M. Werner, Gravitational lensing in the Kerr-Randers optical geometry, *Gen. Rel. Grav.* **44**, 3047 (2012), arXiv:1205.3876 [gr-qc].
- [38] K. Jusufi, A. Övgün, J. Saavedra, Y. Vásquez, and P. González, Deflection of light by rotating regular black holes using the Gauss-Bonnet theorem, *Phys. Rev. D* **97**, 124024 (2018), arXiv:1804.00643 [gr-qc].
- [39] A. Övgün, Weak field deflection angle by regular black holes with cosmic strings using the Gauss-Bonnet theorem, *Phys. Rev. D* **99**, 104075 (2019), arXiv:1902.04411 [gr-qc].
- [40] W. Javed, J. Abbas, and A. Övgün, Effect of the Quintessential Dark Energy on Weak Deflection Angle by Kerr-Newmann Black Hole, *Annals Phys.* **418**, 168183 (2020), arXiv:2007.16027 [gr-qc].
- [41] A. Övgün, Light deflection by Damour-Solodukhin wormholes and Gauss-Bonnet theorem, *Phys. Rev. D* **98**, 044033 (2018), arXiv:1805.06296 [gr-qc].
- [42] A. Övgün, G. Gylchev, and K. Jusufi, Weak Gravitational lensing by phantom black holes and phantom wormholes using the Gauss-Bonnet theorem, *Annals Phys.* **406**, 152 (2019), arXiv:1806.03719 [gr-qc].
- [43] K. Jusufi, N. Sarkar, F. Rahaman, A. Banerjee, and S. Hansraj, Deflection of light by black holes and massless wormholes in massive gravity, *Eur. Phys. J. C* **78**, 349 (2018), arXiv:1712.10175 [gr-qc].
- [44] A. Övgün, K. Jusufi, and I. Sakalli, Gravitational lensing under the effect of Weyl and bumblebee gravities: Applications of Gauss-Bonnet theorem, *Annals Phys.* **399**, 193 (2018), arXiv:1805.09431 [gr-qc].
- [45] A. Övgün, K. Jusufi, and I. Sakalli, Exact traversable wormhole solution in bumblebee gravity, *Phys. Rev. D* **99**, 024042 (2019), arXiv:1804.09911 [gr-qc].
- [46] I. Güllü and A. Övgün, Schwarzschild Like Solution with Global Monopole in Bumblebee Gravity, (2020), arXiv:2012.02611 [gr-qc].
- [47] T. Müller and F. Grave, Catalogue of spacetimes, arXiv preprint arXiv:0904.4184 (2009).